

Supplementary Materials

Breaking the Diffraction Limit in Molecular Imaging by Structured Illumination Mid-Infrared Photothermal Microscopy

Pengcheng Fu^{1†}, Bo Chen^{1†}, Yongqing Zhang¹, Liangyi Chen⁴, Hyeon Jeong Lee^{2,3},

Delong Zhang^{1,5}

¹Zhejiang Key Laboratory of Micro-nano Quantum Chips and Quantum Control, and School of Physics, Zhejiang University, Hangzhou, China.

²College of Biomedical Engineering and Instrument Science, Key Laboratory for Biomedical Engineering of Ministry of Education, Zhejiang University, Hangzhou, China.

³MOE Frontier Science Center for Brain Science & Brain-Machine Integration, Zhejiang University, Hangzhou, China.

⁴New Cornerstone Science Laboratory, State Key Laboratory of Membrane Biology, Beijing Key Laboratory of Cardiometabolic Molecular Medicine, Beijing Laboratory of Biomedical Imaging, Institute of Molecular Medicine, Peking-Tsinghua Center for Life Sciences, School of Future Technology, Peking University, Beijing, China.

⁵Hefei National Laboratory, Hefei 230088, China

[†]These authors contributed equally to this work.

Contents

- 1. Fig. S1 The reconstruction of SIM**
- 2. Fig. S2 The extraction of SIMIP images**
- 3. Fig. S3 The spectrum acquisition of SIMIP**
- 4. Fig. S4 Simulation results of localized temperature profile of a polymer beads**
- 5. Fig. S5 The magnification mismatch of the current SIMIP system**
- 6. Note 1 Sample preparation**
- 7. Note 2 Magnification mismatch of the current SIMIP system**

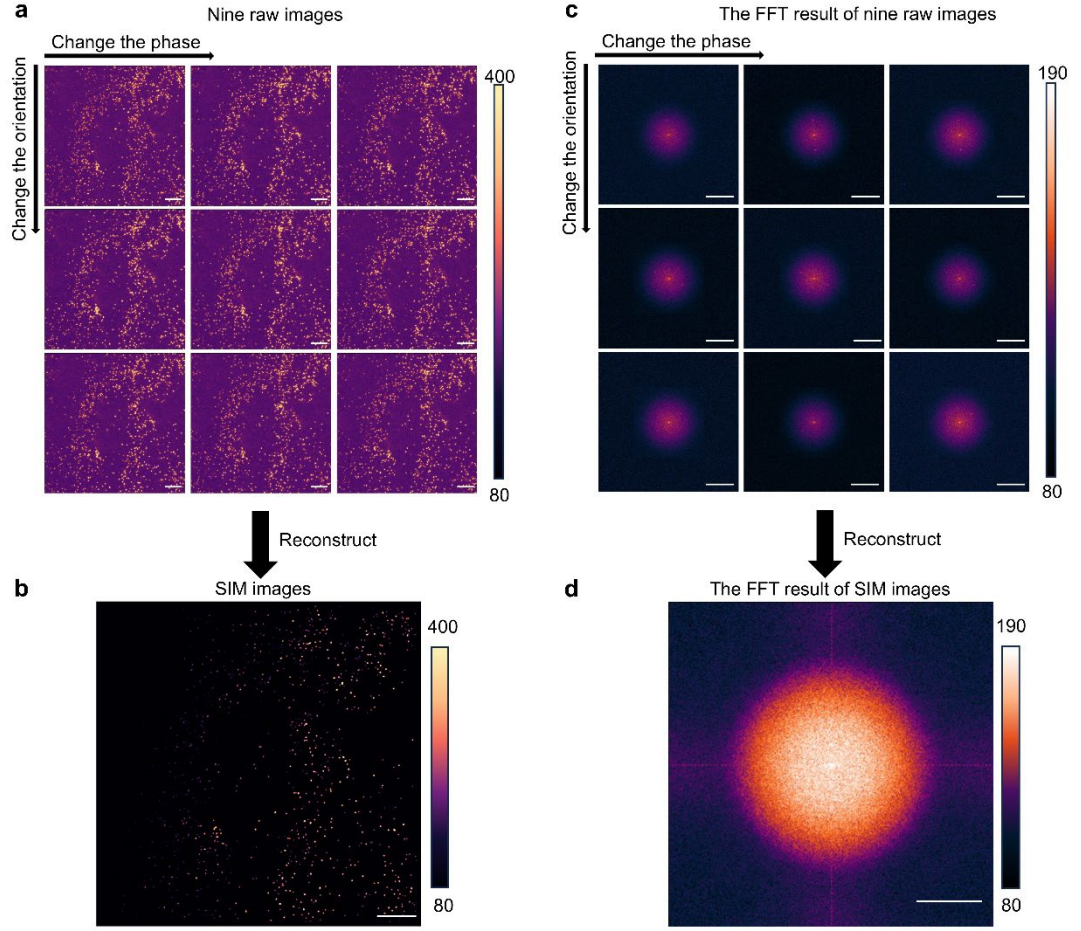


Figure S1. The reconstruction of SIM. (a) The nine raw images used to reconstruct the SIM images. The phase change between the horizontal images and change in stripe orientation between the vertical images. Scale bars: 5 μm . (b) The SIM images after reconstruction. Scale bar: 5 μm . (c) Frequency domain amplitude distribution images of nine raw images used to reconstruct the SIM image. The phase change between the horizontal images and change in stripe orientation between the vertical images. To compared with the frequency domain amplitude distribution image of SIMIP image under the same frame size, Expanded the image around the original image and filled it with random noise. Scale bars: 5 μm^{-1} . (d) Frequency distribution image of SIM image. Scale bar: 5 μm^{-1}

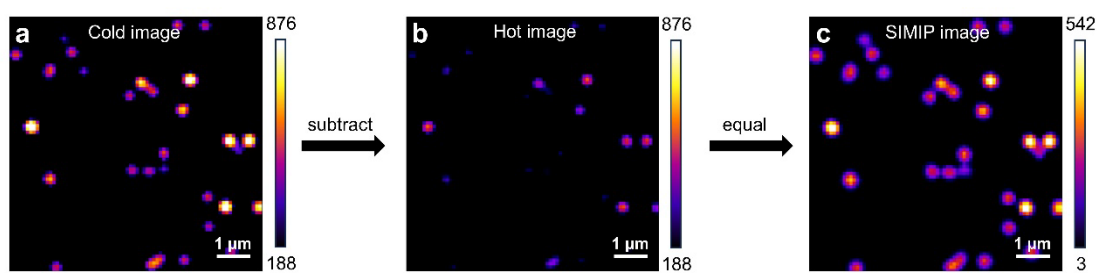


Figure S2. The extraction of SIMIP images. (a) The cold image of 200-nm PMMA beads. (b) The hot image of 200-nm PMMA beads at 1730 cm^{-1} . (c) The SIMIP image derived from subtracting hot image from cold image.

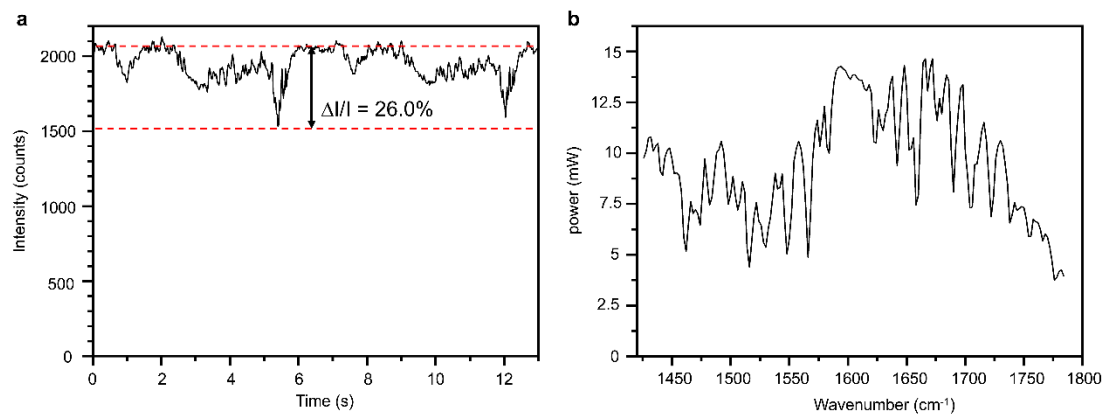


Figure S3. The spectrum acquisition of SIMIP. (a) Raw fluorescence signal trace after baseline correction showing two cycles of wavelength sweeping from fluorescent PMMA beads. The IR wavenumber was tuned repeatedly from 1420 to 1778 cm^{-1} with a tuning speed of 50 cm^{-1}/s . The acquisition interval is 20 ms. (b) Power spectrum of QCL measured in air, the dips are caused by air absorption.

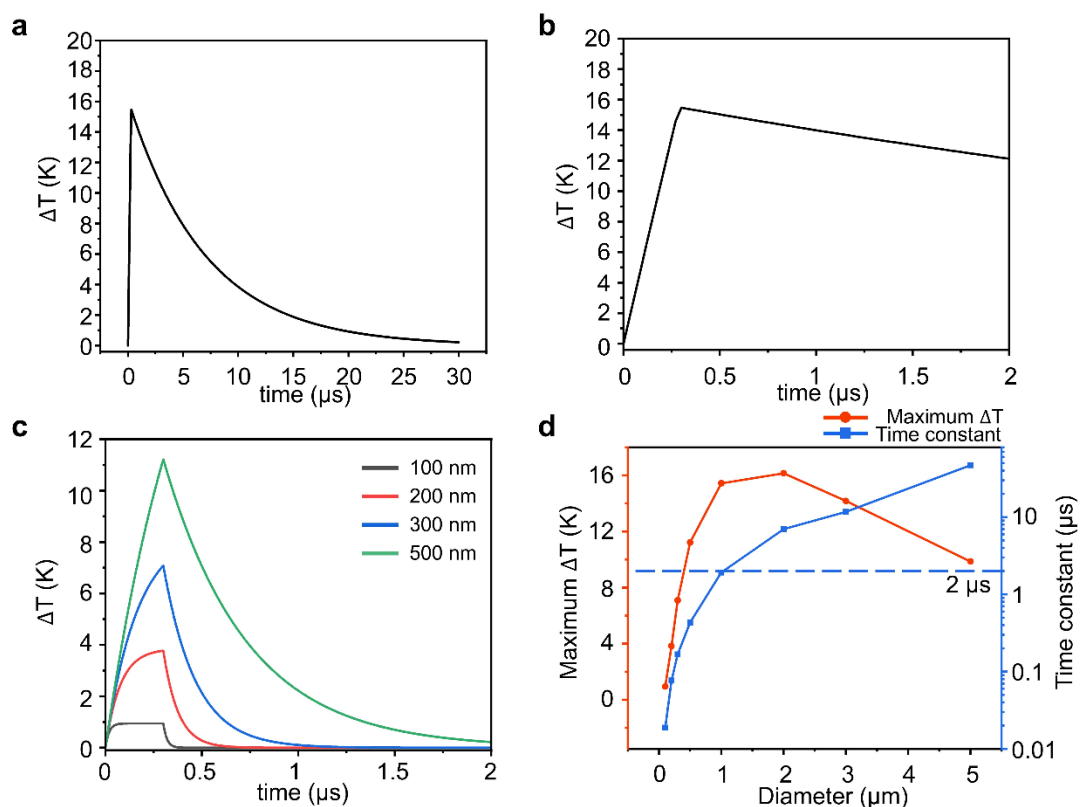


Fig. S4 Simulation results of the localized temperature profile of polymer beads. (a) Simulation of thermodynamic properties of 2- μm PMMA beads. (b) Simulation of thermodynamic properties of 2- μm PMMA beads in an IR period (2 μs). (c) Simulation of thermodynamic properties of PMMA beads with different diameters under a single IR pulse in an IR period. (d) Simulation results of maximum temperature increase and decay time constant of PMMA beads with different diameters under single IR pulse heating.

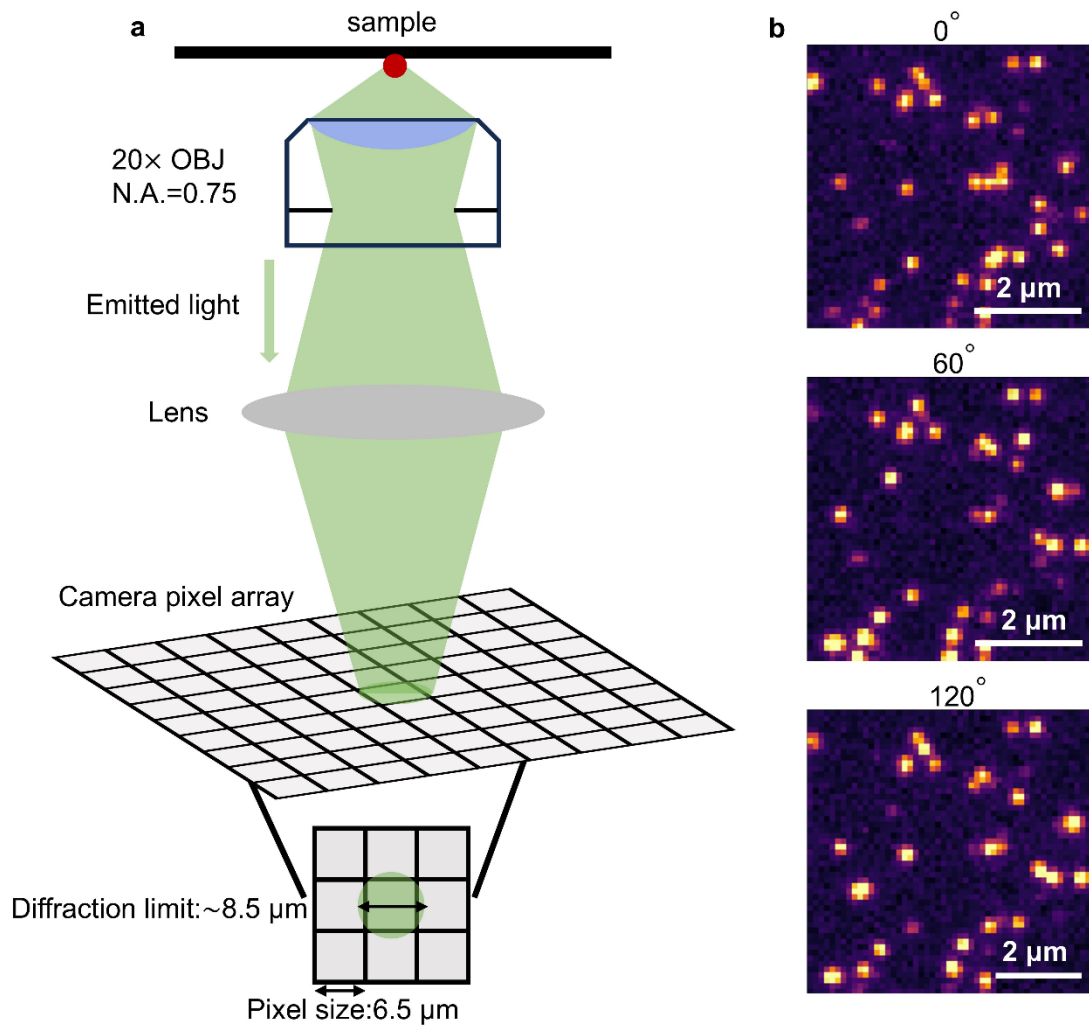


Figure S5. The magnification mismatch of the current SIMIP system. (a) Schematic diagram of the signal collection segment of the microscopic imaging system. (b) Magnified images of the original images with different pattern orientations.

Note 1: Sample preparation

All microsphere stock solutions were diluted 100-fold with distilled water. A 5 μL aliquot was spin-coated onto a CaF_2 slide, air-dried at room temperature for 10-15 minutes, and then sent for imaging.

Note 2: Magnification mismatch of the current SIMIP system

We developed the SIMIP system based on a commercial HIS-SIM platform. For our initial pilot study, we employed a 20 \times air objective (0.75 NA), which provides a theoretical diffraction limit of $d = 0.61 \times \lambda / \text{NA} \times 20 = 8.45 \mu\text{m}$ at an emission wavelength of 520 nm. However, the camera's pixel size of 6.5 \times 6.5 μm fails to meet the Nyquist sampling criterion ($8.45/2 = 4.23 \mu\text{m}$), resulting in degraded resolution. This technical limitation can be addressed in future developments by implementing an objective lens and camera combination with matched magnification.